Few photon switching with slow light in hollow fiber

M. Bajcsy[a], S. Hofferberth[a], V. Balic[a], T. Peyronel[b], M. Hafezi[a], A. S. Zibrov[a], V. Vuletic[b], M.D. Lukin[a]

[a]Physics Department, Harvard University, 17 Oxford St., Cambridge, MA, USA;
[b]Physics Department, MIT, 32 Vassar St., Cambridge, MA, USA;

ABSTRACT

Cold atoms confined inside a hollow-core photonic-crystal fiber with core diameters of a few photon wavelengths are a promising medium for studying nonlinear optical interactions at extremely low light levels. The high electric field intensity per photon and interaction lengths not limited by diffraction are some of the unique features of this system. Here, we present the results of our first nonlinear optics experiments in this system including a demonstration of an all-optical switch that is activated at energies corresponding to few hundred optical photons per pulse.

Keywords: all-optical switch, photonic-crystal fiber, slow light, ultra-cold atoms, electromagnetically induced transparency

1. INTRODUCTION

Interactions between few-photon optical pulses represent the fundamental limit of nonlinear optical science. Reaching this regime has been a long-standing goal, investigated over the last three decades.[1] Additional motivation has recently been provided by potential applications in quantum information science.[2] In general, such nonlinear interactions are very difficult to achieve, as they require a combination of large optical nonlinearity, low photon loss, and tight confinement of the light beams.

In this report, we describe a novel method for achieving such strong nonlinear interactions by taking advantage of coupling between a mesoscopic ensemble of ultra-cold atoms trapped inside a hollow-core photonic crystal fiber (PCF)[3] and photons guided by this fiber. Near atomic resonance, the tight confinement of atoms and photons within few-micron diameter (d) associated with the hollow core of the PCF leads to large interaction probability between a single atom and a single photon of wavelength λ. This probability scales as $p \sim \lambda^2/d^2$, and can, under realistic conditions, approach few percent. With the use of coherent control techniques, such as electromagnetically induced transparency (EIT),[4,5] the optical properties this system can be manipulated by pulses containing $p^{-1} \sim 100$ photons.

Simultaneous implementation of all requirements for few-photon nonlinear optics has until now only been feasible in the context of cavity quantum electrodynamics (QED), where single atoms are trapped within narrow-band, high finesse cavities.[6] Over the last decade, major progress in this area has been achieved, with several experiments demonstrating nonlinear optical phenomena with single intracavity photons.[7–9] However, these experiments remain technologically challenging and must compromise between cavity bandwidth, mirror transmission and atom-photon interaction strength. Consequently, large nonlinearities are accompanied in these systems by substantial losses at the input and output of the cavity. An alternative cavity-free approach uses propagating fields in a PCF. Hollow-core PCF filled with molecular gas have been used for significant enhancements of efficiency in processes such as stimulated Raman scattering[10] and four-wave mixing.[11] Recently, both room-temperature and ultra-cold atoms have successfully been loaded into PCFs[12–14] and observations of EIT with less than a micro-Watt control field have been reported.[12] In our system, the use of cold atoms with purely radiatively broadened atomic transitions further enhances the interaction strength between photons and the atomic ensemble by several orders of magnitude, allowing us to achieve optical switching with control pulses containing only a few hundred photons.

For additional information, e-mail: *bajcsy@fas.harvard.edu or hofferbe@physics.harvard.edu*

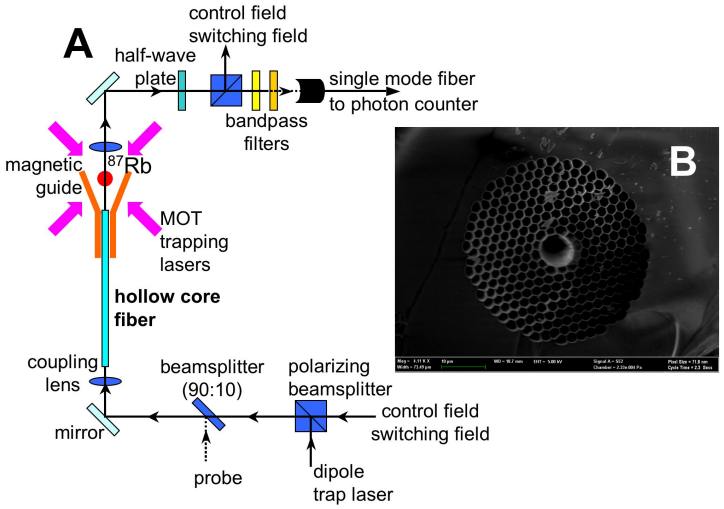

Figure 1. (A) Schematics of the experimental setup. (B) Scanning electron microscope image of the hollow-core PCF

2. EXPERIMENTAL SETUP

Our apparatus (Fig. 1A) makes use of a 3 cm-long piece of single-mode hollow-core PCF vertically mounted inside an ultra-high vacuum chamber. A laser cooled cloud of ^{87}Rb atoms is collected into a magneto-optical trap, focused with a magnetic guide, and loaded into the hollow core of the PCF. Once inside, the atoms are radially confined by a red-detuned dipole trap formed by a single beam guided by the fiber itself. The small diameter of the guided mode allows for strong transverse confinement (trapping frequencies $\omega_t/2\pi \sim 50 - 100\,\mathrm{kHz}$) and deep trapping potential ($\sim 10\,\mathrm{mK}$) at guiding light intensities of a few milliwatts. To probe the atoms in the fiber, we monitor with a single-photon counter the transmission of a very low intensity ($\sim 1\,\mathrm{pW}$) probe beam coupled into the single mode PCF (Fig. 1A).

2.1 Fiber mount

The hollow-core fiber (Fig. 1B)used in the experiment is *HC-800-02* manufactured by *Crystal Fibre*. It has a 7 μm diameter hollow core, and guides light with wavelengths between 780 nm and 900 nm. The fiber is the center-piece of a custom-made, ultra-high vacuum compatible assembly mount that includes coupling and imaging optics, as well as magnetic field generating structures. The fiber piece is held between four current-carrying copper wires, which run parallel to the fiber and fan out upwards in an upside-down pyramid configuration above the fiber (Fig. 2). In addition to these wires, a parallel pair of coils (main axis horizontal, perpendicular to the fiber) is integrated into the fiber mount. Their symmetry center is located slightly above the fiber tip to create a magnetic quadrupole field for the initial stages of the experiment. Besides the current-carrying structures, several optical elements are integrated into the fiber mount as well. Two short focal length lenses allow coupling of light into the guided mode of the fiber ($f = 20\,\mathrm{mm}$ for a lens above the fiber, $f = 4.5\,\mathrm{mm}$ for a lens below). At the fiber top, a single lens with $f = 25\,\mathrm{mm}$ is used for magnified absorption imaging of the atoms near the fiber entrance.

2.2 Loading procedure

Starting point of our fiber loading is a standard six-beam magneto-optical trap (MOT) located approximately 6 mm above the upper tip of the fiber piece (Fig. 2A). The required light fields are provided by three crossing retro-reflected beams with one inch diameter, while the magnetic field is realized by the two circular coils inside the vacuum chamber operated in anti-Helmholtz configuration. During a 1 s loading phase we collect about 10^7 ^{87}Rb atoms at a temperature of $\sim 100\,\mu\mathrm{K}$ in the MOT. After this initial stage, the atoms are optically pumped into the $|F = 2, m_F = 2\rangle$ state and then transferred into a magnetic quadrupole trap formed by the same coils which provide the MOT field. This trap is then adiabatically shifted towards the fiber tip by adding a vertically oriented homogeneous offset field, which displaces the zero field center of the quadrupole trap. In

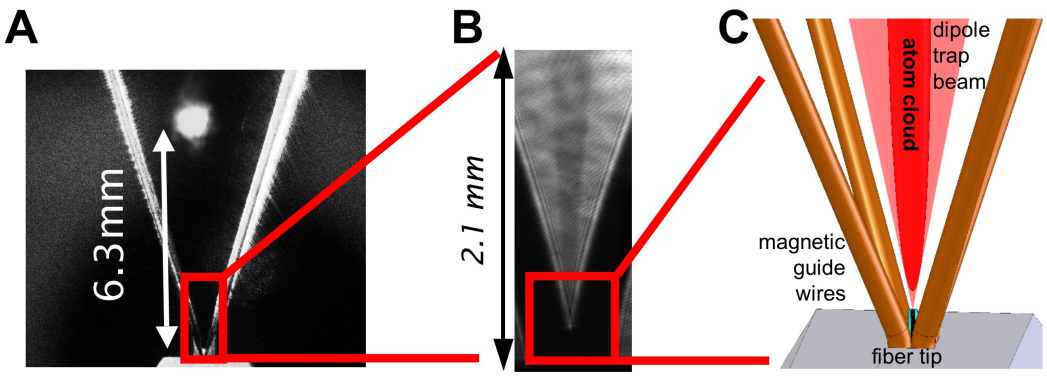

Figure 2. The loading procedure: (A) Atoms collected in a MOT above the fiber. (B) Absorbtion image of the atoms in the magnetic funnel. (C) The atoms are transferred into a red detuned dipole trap inside the fiber.

addition, the magnetic funnel is turned on, creating a transverse quadrupole field, in which the gradient increases with decreasing distance to the fiber. In particular, this transverse gradient reaches $\sim 6\,\mathrm{kG/cm}$ at the fiber tip, resulting in strong radial compression of the magnetic trap. The complete transfer of the magnetic trap towards the fiber takes place over the course of 45 ms. At this point, the atoms are brought within $\sim 100\,\mu\mathrm{m}$ of the fiber tip (Fig. 2B). At the end of the transfer period, all magnetic fields are shut off, while the optical trap beam through the fiber is turned on. We operate the dipole trap slightly red-detuned of the rubidium D2 line, i.e. at $782 - 785\,\mathrm{nm}$. Typically, we use powers of $5 - 8\,\mathrm{mW}$, which is sufficient to provide a trap depth of $\sim 10\,\mathrm{mK}$ inside the fiber. Additionally, since the atoms are pulled toward high light intensity, the diverging beam coming from the fiber tip creates a potential gradient outside the fiber. Based on the beam waist of the fiber mode and the known power in the dipole trap beam, we estimate the capture range of this "optical funnel" as $\sim 100\,\mu\mathrm{m}$, allowing for efficient transfer of the atoms released from the magnetic trap into the fiber (Fig. 2C). Once the atoms are transferred into the optical trap and the magnetic fields are shut off, we wait 5 ms for the atoms to move into the fiber and for transient magnetic fields to vanish before we perform the experiments. Usually, the duration of the actual experiments ranges from 100 to $400\,\mu\mathrm{s}$, during which we modulate the optical trap, as discussed below. The whole cooling, trapping and data collection cycle is repeated every 1.5 s. For the probe transmission scans such as figure 3A, each data point corresponds to a single run of the experiment (or multiple runs in the case of data averaging, as stated in the figure captions). Between these runs, the frequency of the probe laser is changed, and a new atomic sample is prepared in the fiber. This allows for a much longer photon collection time for each probe frequency compared to a full frequency scan during one experiment cycle, reducing the (shot-noise limited) fluctuation of the photon count.

3. ATOMS INSIDE THE FIBER

The signature of atoms inside the PCF are absorption profiles associated with atomic resonance lines. If the atoms are probed inside the dipole trap, we observe a unique profile shown in figure 3A. The dipole trap introduces a power dependent, radially varying AC-Stark shift,[15] which results in broadening and frequency shift of the absorption profile (red data points in Fig. 3A). Comparison with the calculated profile based on the dipole trap parameters verifies that the atoms are loaded inside the fiber. For the experiments described below, we avoid the broadening of the atomic transition by synchronous square-wave modulation of the dipole trap and the probe beam with opposite phase (Fig. 3B) at a rate much higher than the trapping frequency. When using this technique and scanning the probe laser over a particular hyperfine transition, we typically observe a narrowed absorption profile shown in figure 3A (black data points). The shape of this resonance is completely determined by the natural line profile of the transition $T_{nat} = \exp(-\mathrm{OD}/(1+4(\frac{\delta_p}{\Gamma_e})^2))$, where Γ_e is the lifetime of the excited atomic state, $\delta_p = \omega_p - \omega_0$ is the detuning of the probe laser from resonance, and OD is the optical depth as defined below.

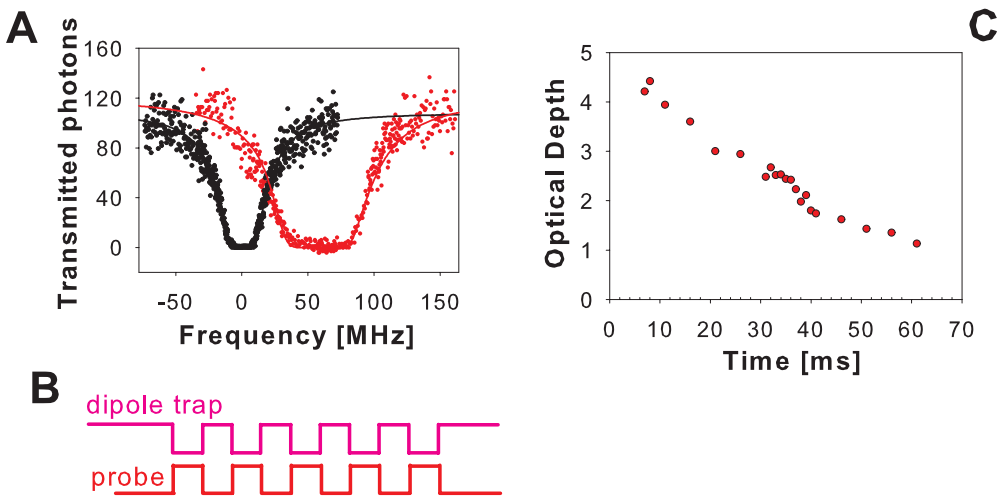

Figure 3. Atoms inside the fiber: (A) Transmission of the fiber as a function of probe frequency with constant dipole trap (broad red data curve centered at $\sim 60MHz$) and with modulated dipole trap (narrow black data curve centered at $0MHz$). (B) Modulation scheme for probe and dipole trap. (C) Optical depth of the atomic cloud inside the fiber as a function of time.

3.1 Optical depth inside the fiber

The optical depth (OD) of a medium describes how much an on-resonant light beam passing through this medium is attenuated. In most experiments, the optical medium is much larger than the light beam, which means that the atomic density over the illuminated area is constant. In this case, the OD can be easily connected to the number of atoms N_{hom} interacting with the light beam: $\mathrm{OD_{hom}} = n_0\sigma_{eg}L = \frac{N_{hom}\sigma_{eg}}{A}$. Here, n_0 is the atomic density, L is the length of the medium, and $A = \pi w_0^2$ is the area of the incident light beam. In our experiment, the atoms are confined within the optical trap created by the guided light inside the fiber. Consequently, the radial extent of the atomic cloud is comparable or smaller than the beam area of the single mode probe light beam propagating through the fiber. To relate the experimentally measured OD to the number of atoms inside the fiber, the exact atomic density distribution enters the OD expression as a geometric prefactor η to the actual number of atoms N_{at}, such that $\mathrm{OD} = \eta\, N_{at}\, (\sigma_{eg}/A)$. The highest value of this prefactor corresponds to all atoms being localized on the axis of the fiber, in which case $\eta = 2$. Note that the optical depth for a given number of atoms inside the fiber does not depend upon the length of the atomic cloud. The measured beam waist of guided light inside the fiber is $w_0 = 1.9 \pm 0.2\,\mu$m. This means that ~ 100 atoms inside the fiber can create an optically dense medium ($OD = 1$). The profile shown in figure 3A yields $OD = 30$, which corresponds to ~ 3000 atoms loaded into the fiber.

3.2 Lifetime of atoms inside the fiber

Once inside the fiber, the atoms are confined by the red detuned dipole trap only in the radial direction, while in the vertical direction they experience a free fall up to when they reach the lower end of the fiber piece. As the atoms move inside the fiber, they are lost from the dipole trap mostly due to collisions with the background gas present due to imperfect vacuum within the PCF core. An example of the measured optical depth of the falling atomic cloud as a function of time is plotted in figure 3C. Here, the zero on the time axis corresponds to the instant when all magnetic fields were shut off. In this measurement each point on the graph corresponds to a newly loaded atomic cloud for which the dipole trap was kept on continuously until the point in time when the OD was measured using the modulation described at the beginning of this section and shown in figure 3B. The 'kink' in the data near 40ms corresponds to the free-falling atoms reaching the lower end of the fiber. Up to this point the atoms decay out of the dipole trap exponentially with a time constant of $\sim 40ms$. We explain the data after the 'kink' as part of the atomic cloud leaving the fiber and part of the cloud reflecting back from

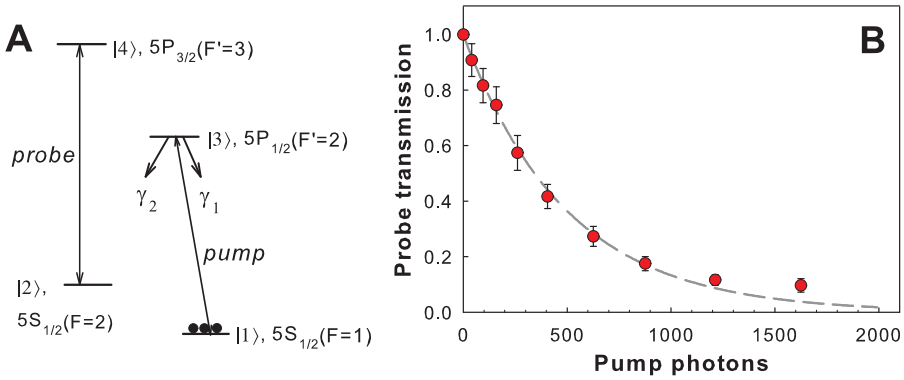

Figure 4. Nonlinear saturation based on incoherent few-photon controlled population transfer: (A) The atomic level scheme and the corresponding hyperfine states (for this level choice $\gamma_2 = \gamma_1$) (B) Transmission of the resonant probe through the fiber as a function of the number of pump photons

the potential change associated with the dipole trap beam exiting from the fiber end into free space. To verify this, we are currently working on detecting the atoms exiting at the lower fiber end.

3.3 Nonlinear saturation based on incoherent few-photon controlled population transfer

To demonstrate the strong atom-light coupling inside the fiber, we now proceed to control the optical properties of our system with light pulses containing a few photons. We first consider nonlinear saturation based on incoherent population transfer in our mesoscopic atomic ensemble. Here, the transmission of the probe beam, coupled to a cycling atomic transition, $|2\rangle \rightarrow |4\rangle$, is controlled via an additional pump beam transferring atoms from an auxiliary state $|1\rangle$ into state $|2\rangle$ (Fig. 4A). Initially, the state $|2\rangle$ is not populated, and the system is transparent for the probe beam. The incident pump beam, resonant with the $|1\rangle \rightarrow |3\rangle$ transition, is fully absorbed by the optically dense atom cloud, exciting the atoms to the $|3\rangle$ state. From there, the atoms can decay into the $|2\rangle$ state, where they then affect the propagation of the probe beam.

In figure 4B, we present the observed transmission of the probe beam as a function of the total number of pump photons sent into the medium. We observe an exponential reduction of the transmission with increasing number of pump photons. In particular, we achieve a 50% reduction of the initial probe transmission for a total number of only 300 pump photons. The efficiency of the incoherent population transfer is limited mainly by the branching ratio of the decay from the excited state $|3\rangle$ to the two ground states $|1\rangle$ and $|2\rangle$. In our case, the probability to decay to the $|2\rangle$ is $p = 1/2$. Hence ~ 150 atoms are transferred into the $|2\rangle$ state, which is sufficient to cause the observed significant absorption of the probe beam.

4. ALL-OPTICAL SWITCHING WITH FEW-HUNDRED PHOTON PULSES

4.1 Electromagnetically induced transparency in with atoms inside the fiber

We now turn to coherent interaction between few atoms and photons in our system. To this end, we demonstrate electromagnetically induced transparency (EIT),[4,5] where intra-atomic coherence induced by a control beam changes the transmission of a probe beam. For this we consider the 3-state 'Lambda' configuration of atomic states shown in figure 5A. In the presence of a strong control field, the weak probe field, resonant with the $|1\rangle \rightarrow |3\rangle$ transition, is transmitted without loss. The essence of EIT is the creation of a coupled excitation of probe photons and atomic spins ("dark-state polariton")[16] that propagates through the atomic medium with greatly reduced group velocity[17] and can be efficiently manipulated.

To demonstrate EIT, we first prepare the atoms in the $F = 1$ ground state, and then probe the medium with a linearly polarized probe tuned to the D1 $F = 1 \rightarrow F' = 1$ transition. In the absence of the control beam, the medium is completely opaque at resonance (Fig. 5C, black data points). In contrast, when a co-propagating control field resonant with the $F = 2 \rightarrow F' = 1$ transition is added, the atomic ensemble becomes

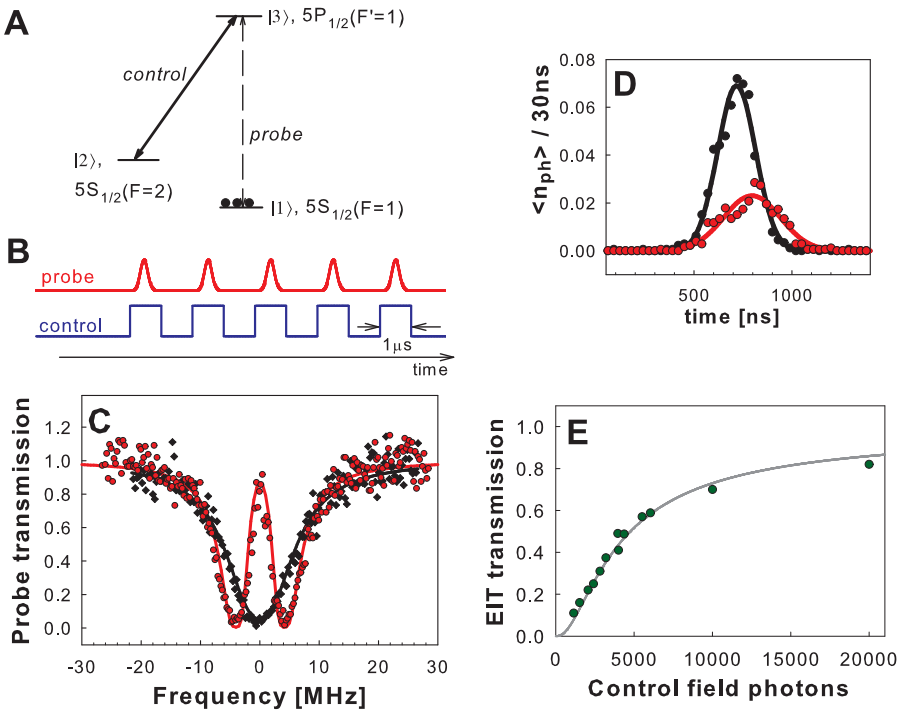

Figure 5. Electromagnetically induced transparency with atoms inside the fiber: (A) The atomic level scheme and the corresponding hyperfine states. (B) Both probe and control field are broken into a set of $\sim$ 100 synchronized pulses sent through the fiber during the off-times of the dipole trap. (C) Transmission of the probe light through the fiber as a function of detuning from the resonance in the presence of the control field (red data). The black data shows probe transmission without the control field. (D) Individual probe pulse shape and delay. Here, $\langle n_{ph} \rangle$ represents the average number of photons detected in a 30 ns time bin. The reference pulse (black) is obtained without the presence of atoms, while the EIT pulse (red) is delayed. (E) Observed transmission of the probe pulses on resonance as a function of average number of photons in the 1 μs control field pulse and the prediction (grey line) obtained by evaluating eq. (2).

transparent near the probe resonance (Fig. 5C, red data points). Figure 5D shows the individual pulse shape and its transmission and delay due to reduced group velocity v_g inside the atomic medium. For a probe pulse of half-width $t_p \sim 150$ ns we observe a group delay t_d approaching 100 ns, corresponding to reduction of group velocity to $v_g \approx 3$ km/s. Finally, figure 5E shows the resonant probe transmission as a function of the average number of photons contained in each control field pulse. Remarkably, control pulses containing $\sim 10^4$ photons are sufficient to achieve almost complete transparency of an otherwise opaque system.

4.2 An all-optical switch

The sensitive nature of the quantum interference underlying EIT enables strong non-linear coherent interaction between the dark-state polariton and additional light fields, which can be viewed as an effective photon-photon interaction.[18–20] An efficient nonlinear optical switch can be realized by adding to the EIT 'Lambda'-system a switch field coupling the state $|2\rangle$ to an excited state $|4\rangle$(Fig. 6A), as proposed by Harris and Yamamoto.[21] In this scheme, the switching photons interact with flipped atomic spins within the slow dark-state polariton, causing a simultaneous absorption of a probe and a switch photon.[22–24]

In our experiment, an additional switching field on the D2 $F = 2 \rightarrow F' = 3$ transition (Fig. 6A) controls the transmission through the EIT medium. Switching is achieved when all three involved light fields (probe, control and switching field) are overlapping in time (Fig. 6B). As shown in Figure 6C, in the absence of the switching field (red data), we observe high transmission of the probe beam on resonance due to EIT. When the switch field is turned on, this transmission is reduced. The strength of the reduction depends on the switch field intensity, which, for a fixed switch pulse length, is determined by the number of photons contained in the switch pulse

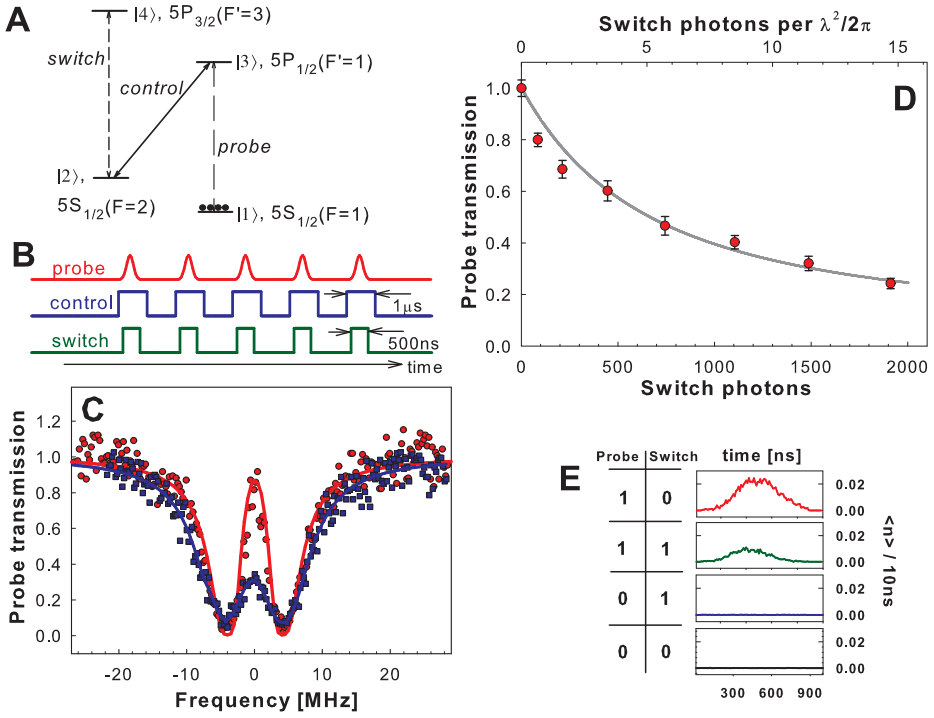

Figure 6. An all-optical switch: (A) The atomic level scheme with corresponding hyperfine states. (B) Probe, control and switch fields are broken into a set of ~ 100 synchronized pulses sent through the fiber during the off-times of the dipole trap. (C) Probe transmission through the fiber without (red) and with (blue) the switch field present. Solid lines are fits of equation (2). (D) Observed transmission versus average number of switch photons per pulse. The solid grey line is the prediction based on equation (2). The transmission is normalized to the EIT transmission in the absence of the switch photons. (E) Truth table of the switch, showing the detected photons in the output port of the switch system as a function of the presence of the probe and switch field pulses. Data are presented for probe pulses containing on average ~ 2 photons and $\sim 1/e$ attenuation of transmission in the presence of the switch photons.

(Fig. 6D). Experimentally, we observe best switching results for switch pulses of length $t_s \approx t_p + t_d$. We find a 50% reduction of the initial transmission for a total number of ~ 700 switch photons per pulse. Figure 6E presents the truth table of our switch. In the case of no probe pulse (0/0 and 0/1 settings of the switch) only background noise from the control field is detected, which is orders of magnitude smaller than the single photon per probe pulse.

4.3 Analysis of pulse transmission

We now turn to the detailed analysis of the nonlinear behavior of our atomic medium. In the case when the resonant control and switching pulses are longer than the weak probe pulse, the effect of the atomic medium on such probe pulses with carrier frequency ω_p is given by $\mathcal{E}_{\rm out}(t) = \frac{1}{\sqrt{2\pi}} \int {\rm d}\omega\, \mathcal{E}_{\rm in}(\omega)\, e^{\imath \frac{\rm OD}{2} f(\omega)}\, e^{-\imath\omega t}$, where $\mathcal{E}_{\rm in}(\omega)$ is the Fourier transform of the slowly varying envelope $\mathcal{E}_{in}(t)$ of the probe pulse. The frequency dependent atomic response to probe light $f(\omega)$ is given by[19,21]

$$f(\omega) = \frac{\gamma_{13}\left(|\Omega_s|^2 - 4\delta_{12}\delta_{24}\right)}{\delta_{24}\left(4\delta_{12}\delta_{13} - |\Omega_c|^2\right) - \delta_{13}\,|\Omega_s|^2}. \qquad (1)$$

Here, $\Omega_{s,c} = \frac{\mu_{s,c} E_{s,c}}{\hbar}$ are the Rabi frequencies of the switch and control fields, with $\mu_{s,c}$ being the respective dipole matrix elements. The complex detunings δ_{ij} are defined as $\delta_{ij} = \delta_p + \imath\gamma_{ij}$, with γ_{ij} being the dephasing rates between levels i, j, while $\delta_p = \omega_p + \omega - \omega_{13}$, where ω_{13} is the frequency of the $|1\rangle \rightarrow |3\rangle$ transition. The

number of input and output photons is given by $N_{in,out} = \int \mathrm{d}t\ |\mathcal{E}_{\mathrm{in,out}}(t)|^2$. In what follows, we consider input pulses with Gaussian envelope $\mathcal{E}_{\mathrm{in}}(t) \sim e^{-\frac{t^2}{2t_p^2}}$, in which case the transmission through our atomic medium is

$$T(\omega_p, \mathrm{OD}) = \frac{N_{out}}{N_{in}} = \frac{t_p}{\sqrt{\pi}} \int \mathrm{d}\omega\, e^{-t_p^2\omega^2}\, e^{-\mathrm{OD}\,\mathrm{Im} f(\omega)}. \tag{2}$$

We fit expression (2) to the observed absorption profiles such as the ones shown in figures 5C and 6C to extract the control and switch Rabi frequencies, optical depth and ground state decoherence rate. We next use these parameters to compare our observed EIT and coherent switch data to the theoretical prediction. The solid line in Figure 5E shows the calculated EIT transmission as a function of control pulse photons. Similarly, the solid line in figure 6D shows the on-resonance attenuation of the probe pulse as a function of switch photons. In both cases, we find excellent agreement between our experimental data and the theoretical model.

In the relevant case of on resonant probe field, equation (1) can be approximated by

$$T = \frac{\exp\left(-N_s \left(\frac{\mu_s}{\mu_p}\right)^2 \frac{3}{\pi}\frac{\lambda^2}{A}\frac{t_d}{t_p+t_d}\right)}{\sqrt{1+\frac{16t_d^2}{\mathrm{OD}\,t_p^2}}}. \tag{3}$$

Here, N_s is the number of switch photons. Furthermore, we have assumed $\Omega_s \ll \Omega_c$, $\gamma_{12} = 0$, $\gamma_{13} \approx \gamma_{24}$ and used $t_d = L/v_g = \frac{\mathrm{OD}\gamma_{13}}{|\Omega_c|^2}$, with L being the length of the medium. For the investigated case of a relatively weak probe transition and resulting OD ≈ 3, the delay time is small ($t_d \sim t_p$) and the probe pulse is never fully stored inside the medium. If the OD is increased (either by improving the atom loading efficiency or using a stronger probe transition), $t_d \gg t_p$ and the whole probe pulse is contained inside the medium as a dark state polariton in a mostly atomic form. In this case, it follows from equation (3) that $N_s \sim \frac{A}{\lambda^2}$ switch photons cause $1/e$ attenuation of the probe pulse. This ideal limit can be easily understood. In the case of a single slow probe photon, the polariton contains only a single atomic spin at any time. Consequently, absorption of a single switch photon, which occurs with probability $p \sim \lambda^2/A$, is required to destroy this coherent atomic excitation.

5. OUTLOOKS

Our experimental demonstrations introduce a novel physical system that opens up unique prospects in quantum and nonlinear optics. For example, our system can be used to implement efficient photon counting[25,26] by combining photon storage with spin-flipped atom interrogation via the cycling transition. Further improvements in nonlinear optical efficiency are possible by either simultaneously slowing down a pair of pulses to enable long interaction time[27] or using stationary-pulse techniques.[28] In the later case, a standing wave control field formed by two counter-propagating beams is used to form an EIT Bragg grating in which the probe pulse can be completely stopped with non-vanishing photonic component. In particular, application of this scheme inside the PCF has been proposed for single photon controlled switching through an interaction of single-photon stationary light pulses, with probability of interaction between two single photons scaling as $\sim OD\lambda^2/A$.[29] With relatively modest improvement in atom loading resulting in optical depth $OD > 100$, achieving deterministic nonlinear switching with two guided photons appears within reach. Finally, the present demonstration opens up the possibility to create strongly interacting many-body photon states,[30] which may give new insights into the physics of non-equilibrium strongly correlated systems.

ACKNOWLEDGMENTS

We would like to thank Yiwen Chu and David Brown for their help in building the electronics for the experiment. This work was supported by MIT-Harvard Center for Ultracold Atoms, NSF, DARPA and Packard Foundation.

REFERENCES

[1] Boyd, R., *Nonlinear Optics*, Academic Press, New York (1992).

[2] Bouwmeester, D., Ekert, A. K., and Zeilinger, A., *The Physics of Quantum Information*, Springer, New York (2000).

[3] Cregan, R., Mangan, B., Knight, J., Birks, T., Russell, P., Roberts, P., and Allan, D., "Single-mode photonic band gap guidance of light in air," *Science* **285**(5433), 1537 – 1539 (1999).

[4] Harris, S., "Electromagnetically induced transparency," *Phys. Today* **50**, 36 – 42 (1997).

[5] Fleischhauer, M., Imamoğlu, A., and Marangos, J., "Electromagnetically induced transparency: Optics in coherent media," *Rev. Mod. Phys.* **77**, 633 (2005).

[6] Dayan, B., Parkins, A. S., Aok, T., Ostby, E., Vahala, K., and Kimble, H., "A photon turnstile dynamically regulated by one atom," *Science* **319**(5866), 1062–1065 (2008).

[7] Birnbaum, K. M., Boca, A., Miller, R., Boozer, A. D., Northup, T. E., and Kimble, H. J., "Photon blockade in an optical cavity with one trapped atom," *Nature* **436**, 87 (2005).

[8] Wilk, T., Webster, S. C., Kuhn, A., and Rempe, G., "Single-atom single-photon quantum interface," *Science* **317**, 488 – 490 (2007).

[9] Fushman, I., Englund, D., Faraon, A., Stoltz, N., Petroff, P., and Vuckovic, J., "Controlled phase shifts with a single quantum dot," *Science* **320**(5877), 769–772 (2008).

[10] Benabid, F., Knight, J., Antonopoulos, G., and Russell, P., "Stimulated Raman scattering in hydrogen-filled hollow-core photonic crystal fiber," *Science* **298**, 399–402 (OCT 11 2002).

[11] Konorov, S. O., Fedotov, A. B., and Zheltikov, A. M., "Enhanced four-wave mixing in a hollow-core photonic-crystal fiber," *Opt. Lett.* **28**, 1448 – 1450 (2003).

[12] Ghosh, S., Bhagwat, A. R., Renshaw, C. K., Goh, S., Gaeta, A. L., and Kirby, B. J., "Low-light-level optical interactions with rubidium vapor in a photonic band-gap fiber," *Phys. Rev. Lett.* **97**(2), 023603 (2006).

[13] Takekoshi, T. and Knize, R. J., "Optical guiding of atoms through a hollow-core photonic band-gap fiber," *Phys. Rev. Lett.* **98**(21), 210404 (2007).

[14] Christensen, C. A., Will, S., Saba, M., Jo, G.-B., Shin, Y.-I., Ketterle, W., and Pritchard, D., "Trapping of ultracold atoms in a hollow-core photonic crystal fiber," *Physical Review A (Atomic, Molecular, and Optical Physics)* **78**(3), 033429 (2008).

[15] Grimm, R., Weidemuller, M., and Ovchinnikov, Y., "Optical dipole traps for neutral atoms," *Adv. in Atomic, Molec., and Opt. Phys.* **42**, 95–170 (2000).

[16] Fleischhauer, M. and Lukin, M. D., "Dark-state polaritons in electromagnetically induced transparency," *Phys. Rev. Lett.* **84**, 5094 – 5097 (2000).

[17] Hau, L., Harris, S., Dutton, Z., and Behroozi, C., "Light speed reduction to 17 metres per second in an ultracold atomic gas," *Nature* **397**(6720), 594–598 (1999).

[18] Harris, S., Field, J., and Imamoğlu, A., "Nonlinear optical processes using electromagnetically induced transparency," *Phys. Rev. Lett.* **64**, 1107 (1990).

[19] Schmidt, H. and Imamoğlu, A., "Giant Kerr nonlinearities obtained by electromagnetically induced transparency," *Opt. Lett.* **21**, 1936 (1996).

[20] Lukin, M. and Imamoğlu, A., "Controlling photons using electromagnetically induced transparency," *Nature* **413**(6853), 273–276 (2001).

[21] Harris, S. and Yamamoto, Y., "Photon switching by quantum interference," *Phys. Rev. Lett.* **81**, 3611 (1998).

[22] Yan, M., Rickey, E., and Zhu, Y., "Observation of absorptive photon switching by quantum interference," *Phys. Rev. A* **64**, 041801(R) (2001).

[23] Braje, D., Balic, V., Yin, G., and Harris, S., "Low-light-level nonlinear optics with slow light," *Phys. Rev. A* **68**, 041801(R) (2003).

[24] Chen, Y., Tsai, Z., Liu, Y., and Yu, I., "Low-light-level photon switching by quantum interference," *Opt. Lett.* **30**, 3207 (2005).

[25] Imamoğlu, A., "High efficiency photon counting using stored light," *Phys. Rev. Lett.* **89** (OCT 14 2002).

[26] James, D. and Kwiat, P., "Atomic-vapor-based high efficiency optical detectors with photon number resolution," *Phys. Rev. Lett.* **89**, 183601 (2002).

[27] Lukin, M. and Imamoğlu, A., "Nonlinear optics and quantum entanglement of ultraslow single photons," *Phys. Rev. Lett.* **84**, 1419 (2000).

[28] Bajcsy, M., Zibrov, A. S., and Lukin, M. D., "Stationary pulses of light in an atomic medium," *Nature* **426**, 638–641 (2003).

[29] André, A., Bajcsy, M., Zibrov, A. S., and Lukin, M. D., "Nonlinear optics with stationary pulses of light," *Physical Review Letters* **94**(6), 063902 (2005).

[30] Chang, D., Gritsev, V., Morigi, G., Vuletic, V., Lukin, M., and Demler, E., "Crystallization of strongly interacting photons in a nonlinear optical fiber," *Nature Physics* **4**, 884 (2008).